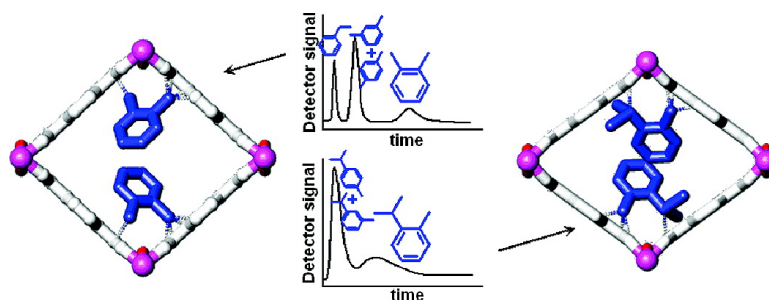Article

Selective Adsorption and Separation of *ortho*-Substituted Alkylaromatics with the Microporous Aluminum Terephthalate MIL-53

Luc Alaerts, Michael Maes, Lars Giebeler, Pierre A. Jacobs, Johan A. Martens, Joeri F. M. Denayer, Christine E. A. Kirschhock, and Dirk E. De Vos

More About This Article

Additional resources and features associated with this article are available within the HTML version:

- Supporting Information
- Access to high resolution figures
- Links to articles and content related to this article
- Copyright permission to reproduce figures and/or text from this article

View the Full Text HTML

Selective Adsorption and Separation of *ortho*-Substituted Alkylaromatics with the Microporous Aluminum Terephthalate MIL-53

Luc Alaerts,[†] Michael Maes,[†] Lars Giebeler,[†] Pierre A. Jacobs,[†] Johan A. Martens,[†] Joeri F. M. Denayer,[‡] Christine E. A. Kirschhock,[†] and Dirk E. De Vos*,[†]

Centre for Surface Chemistry and Catalysis, Katholieke Universiteit Leuven, Kasteelpark Arenberg 23, 3001 Leuven, Belgium, and Department of Chemical Engineering, Vrije Universiteit Brussel, Pleinlaan 2, 1050 Brussel, Belgium

Received April 15, 2008; E-mail: dirk.devos@biw.kuleuven.be

Abstract: The metal−organic framework MIL-53(Al) was tested for selective adsorption and separation of xylenes and ethylbenzene, ethyltoluenes, and cymenes using batch, pulse chromatographic, and breakthrough experiments. In all conditions tested, MIL-53 has the largest affinity for the *ortho*-isomer among each group of alkylaromatic compounds. Separations of the *ortho*-compounds from the other isomers can be realized using a column packed with MIL-53 crystallites. As evidenced by Rietveld refinements, specific interactions of the xylenes with the pore walls of MIL-53 determine selectivity. In comparison with the structurally similar metal−organic framework MIL-47, the selectivities among alkylaromatics found for MIL-53 are different. Separation of ethyltoluene and cymene isomers is more effective on MIL-53 than on MIL-47; the pores of MIL-53 seem to be a more suitable environment for hosting the larger ethyltoluene and cymene isomers than those of MIL-47.

1. Introduction

Metal−organic frameworks (MOFs) are an emerging class of microporous crystalline materials. They consist of clusters or chains of metal ions connected by organic ligands, often aromatic polycarboxylic acids. As the metal ions are, in most cases, coordinatively saturated by these ligands, the pore walls are largely organic in composition.[1−6] Before now, MOFs have been applied as catalysts,[7,8] luminescent and magnetic materials,[9,10] and drug delivery vehicles.[11] One of the most promising applications for MOFs seems to be their use as adsorbents. MOFs have frequently been investigated for storage of perma-

nent gases like hydrogen, methane, or carbon dioxide.[12−21] Adsorption of larger organic compounds currently is a rarely explored field.[22−25] Many MOFs are available now with sufficiently large pore windows and cages, and in most of them

[†] Katholieke Universiteit Leuven.

[‡] Vrije Universiteit Brussel.

(1) Rowsell, J.; Yaghi, O. *Microporous Mesoporous Mater.* **2004**, *73*, 3–14.

(2) Janiak, C. *Dalton Trans.* **2003**, 2781–2804.

(3) Chui, S.; Lo, S.; Charmant, J.; Orpen, A.; Williams, I. *Science* **1999**, *283*, 1148–1150.

(4) Férey, G.; Mellot-Draznieks, C.; Serre, C.; Millange, F.; Dutour, J.; Surblé, S.; Margiolaki, I. *Science* **2005**, *309*, 2040–2042.

(5) Loiseau, T.; Serre, C.; Huguenard, C.; Fink, G.; Taulelle, F.; Henry, M.; Bataille, T.; Férey, G. *Chem. Eur. J.* **2004**, *10*, 1373–1382.

(6) Barthelet, K.; Marrot, J.; Riou, D.; Férey, G. *Angew. Chem., Int. Ed.* **2002**, *41*, 281–284.

(7) Alaerts, L.; Séguin, E.; Poelman, H.; Thibault-Starzyk, F.; Jacobs, P.; De Vos, D. *Chem. Eur. J.* **2006**, *12*, 7353–7363.

(8) Horcajada, P.; Surble, S.; Serre, C.; Hong, D.; Seo, Y.; Chang, J.; Greneche, J.; Margiolaki, I.; Ferey, G. *Chem. Commun.* **2007**, 2820–2822.

(9) Guillou, N.; Livage, C.; Drillon, M.; Férey, G. *Angew. Chem., Int. Ed.* **2003**, *42*, 5314–5317.

(10) Li, Z.; Zhu, G.; Guo, X.; Zhao, X.; Jin, Z.; Qiu, S. *Inorg. Chem.* **2007**, *46*, 5174–5178.

(11) Horcajada, P.; Serre, C.; Vallet-Regi, M.; Sebban, M.; Taulelle, F.; Ferey, G. *Angew. Chem., Int. Ed.* **2006**, *45*, 5974–5978.

(12) Latroche, M.; Surble, S.; Serre, C.; Mellot-Draznieks, C.; Llewellyn, P.; Lee, J.; Chang, J.; Jhung, S.; Ferey, G. *Angew. Chem., Int. Ed.* **2006**, *45*, 8227–8231.

(13) Bourrelly, S.; Llewellyn, P.; Serre, C.; Millange, F.; Loiseau, T.; Férey, G. *J. Am. Chem. Soc.* **2005**, *127*, 13519–13521.

(14) Panella, B.; Hirscher, M.; Puetter, H.; Mueller, U. *Adv. Funct. Mater.* **2006**, *16*, 520–524.

(15) Férey, G.; Latroche, M.; Serre, C.; Millange, F.; Loiseau, T.; Percheron-Guégan, A. *Chem. Commun.* **2003**, 2976–2977.

(16) Serre, C.; Bourrelly, S.; Vimont, A.; Ramsahye, N.; Maurin, G.; Llewellyn, P.; Daturi, M.; Filinchuk, Y.; Leynaud, O.; Barnes, P.; Férey, G. *Adv. Mater.* **2007**, *19*, 2246.

(17) Liu, Y.; Eubank, J. F.; Cairns, A. J.; Eckert, J.; Kravtsov, V. C.; Luebke, R.; Eddaoudi, M. *Angew. Chem., Int. Ed.* **2007**, *46*, 3278–3283.

(18) Perles, J.; Iglesias, M.; Martín-Luengo, M.; Ángeles Monge, M.; Ruiz-Valero, C.; Snejko, N. *Chem. Mater.* **2005**, *17*, 5837–5842.

(19) Rosi, N.; Eckert, J.; Eddaoudi, M.; Vodak, D.; Kim, J.; O'Keeffe, M.; Yaghi, O. *Science* **2003**, *300*, 1127–1129.

(20) Sun, D.; Ma, S.; Ke, Y.; Collins, D.; Zhou, H. *J. Am. Chem. Soc.* **2006**, *128*, 3896–3897.

(21) Eddaoudi, M.; Kim, J.; Rosi, N.; Vodak, D.; Wachter, J.; O'Keeffe, M.; Yaghi, O. *Science* **2002**, *295*, 469–472.

(22) Pan, L.; Olson, D.; Ciemnolonski, L.; Heddy, R.; Li, J. *Angew. Chem., Int. Ed.* **2006**, *45*, 616–619.

(23) Wang, X.; Liu, L.; Jacobson, A. *Angew. Chem., Int. Ed.* **2006**, *45*, 6499–6503.

(24) Nandini Devi, R.; Edgar, M.; Gonzalez, J.; Slawin, A. M. Z.; Tunstall, D. P.; Grewal, P.; Cox, P. A.; Wright, P. A. *J. Phys. Chem. B* **2004**, *108*, 535–543.

(25) Huang, L.; Wang, H.; Chen, J.; Wang, Z.; Sun, J.; Zhao, D.; Yan, Y. *Microporous Mesoporous Mater.* **2003**, *58*, 105–114.

(26) *Ullmann's Encyclopedia of Industrial Chemistry*, 6th Ed.; John Wiley & Sons: New York, 2006; electronic release.

an important fraction of the pore walls consists of aromatic rings.[1−25] For these reasons, we focused on adsorption of alkylaromatics in the pores of MOFs.

In industry, the most important alkylaromatic compounds are the C_8 alkylaromatics, such as xylenes and ethylbenzene. The pure isomers are of high value. For instance, *p*-xylene is oxidized to terephthalic acid for poly(ethylene terephthalate) (PET) production; ethylbenzene is dehydrogenated to styrene for polystyrene production.[26] Their separation is a technical challenge, due to the similarity of their boiling points and dimensions.[26,27] The preferred way to achieve separation of C_8 alkylaromatics is based on the different confinement of the isomers in the nanoscaled pore system of an adsorbent. The cages of faujasite zeolites are well suited for this purpose, especially when exchanged with cations like Na^+, K^+, or Ba^{2+}. Such zeolites are currently used in industrial adsorptive separation processes.[27−35] Other alkylaromatic isomers are the ethyltoluenes and the cymenes, which possess as substituents a methyl group next to an ethyl or an isopropyl group. They are used as solvents or intermediates, but on a much smaller scale than the C_8 alkylaromatics.[26] Due to the larger dimensions of these compounds, separation can be accomplished with zeolite adsorbents exploiting shape-selectivity. Ethyltoluene isomers can be separated in a two-step process in which a ferrierite adsorbent bed first retains *p*-ethyltoluene from the ethyltoluene feed, and subsequently *m*-ethyltoluene is selectively retained by a silicalite adsorbent bed.[36] A major industrial pathway using *m*- and *p*-cymene is the oxidation to the corresponding cresol isomers. A feed with a minimized *o*-cymene concentration is preferred for this process, as this particular compound is difficult to oxidize and inhibits the oxidation of the other isomers. Pure cymene isomers can be obtained via the Cymex process using a 13X molecular sieve.[37]

In this work, selective adsorption and separation of xylenes and ethylbenzene, ethyltoluenes, and cymenes is investigated using MIL-53(Al). This MOF consists of infinite chains of octahedra formed by coordination of Al^{III} by terephthalate and $OH^−$ groups. The terephthalate ligands point in four directions. In this way, one-dimensional lozenge-shaped pores with diameters of ca. 8.5 Å are formed, with walls mainly consisting of aromatic rings. The structure has a remarkable breathing behavior: the lattice contracts, for instance, upon adsorption of water or carbon dioxide.[5,16] In the present work, an experimental approach combining batch and column experiments is used to probe the potential of MIL-53(Al) for separations of alkylaromatics and to investigate the mechanisms determining adsorption

selectivities. The adsorbates were localized inside the MIL-53 host by Rietveld refinements of X-ray powder diffraction (XRD) patterns of saturated MIL-53 samples. The adsorption properties of MIL-53 are eventually compared with those of MIL-47, a similarly constructed MOF consisting of V^{IV}, $O^{2−}$, and terephthalate.[6]

2. Experimental Section

2.1. Synthesis of Materials. The hydrothermal synthesis of MIL-53(Al)*as* (*as*-synthesized) was based on a literature procedure.[5] Typically, 1.88 g of $Al(NO_3)_3 \cdot 9H_2O$ (Riedel-de Haën, 98%), 0.41 g of terephthalic acid (Acros, 99+%), and 3.58 g of H_2O were mixed in a 30 mL Teflon-lined stainless steel autoclave, which was heated at 493 K for 3 days. After cooling down, washing with H_2O, and drying at 333 K, the white powder was calcined in shallow beds in a muffle furnace in air at 603 K for 3 days to remove the incorporated terephthalic acid from the pores. The obtained material had a pore volume of 0.50 mL $g^{−1}$ and a specific surface of 940 m^2 $g^{−1}$. XRD revealed a single-phase material before adsorption. Crystals between 2 and 10 μm were observed with scanning electron microscopy (SEM). Before use in adsorption experiments, the MIL-53 powder was dried overnight at 473 K to convert the *low-temperature* form (MIL-53*lt*) with adsorbed water to the open *high-temperature* form (MIL-53*ht*).[5]

The hydrothermal synthesis of MIL-47*as* was based on a literature procedure.[6] Typically, 1.224 g of VCl_3 (Acros, 97%), 0.323 g of terephthalic acid (Acros, 99+%), and 14.00 g of H_2O were mixed in a 30 mL Teflon-lined steel autoclave, which was heated at 473 K for 4 days. Calcination of MIL-47*as* was typically performed by treating 16 mg $cm^{−2}$ of the material in shallow beds of 42 cm^2 in a muffle furnace in air at 573 K for 21.5 h to remove the occluded terephthalic acid from the pores and to oxidize V^{III} to V^{IV}. The obtained material had a pore volume of 0.32 mL $g^{−1}$ and a specific BET surface of 750 m^2 $g^{−1}$. In this single-phase material, orthorhombic crystals ranging from 0.25 to 2.0 μm were observed by SEM. As the material is hydrophobic, no thermal treatment was performed before use in adsorption experiments.

2.2. Adsorption Experiments. Liquid-phase batch experiments were based on a literature procedure.[38,39] For each experiment, a 1.8 mL vial with 0.025 g of pretreated adsorbent (see section 2.1) and an empty reference vial were filled with a solution of alkylaromatics in hexane and stirred for 2 h at 298 K. From gas chromatographic (GC) analysis, equilibrium and initial concentrations of aromatics were determined. The differences between these pairs of concentration values were used directly for the calculation of adsorbed amounts, expressed as weight percentages, as moles per gram, or as number of molecules adsorbed per unit cell (calculation based on the ideal crystal structure of MIL-53; the composition of one unit cell is $[Al(OH)(O_2C-C_6H_4-CO_2)]_4$). For competitive experiments, selectivities $\alpha_{i,j}$ were calculated using eq 1,

$$\alpha_{i,j} = \left(\frac{q_i}{q_j}\right) \times \left(\frac{c_j}{c_i}\right) \qquad (1)$$

with q_i and q_j the amounts (mol $g^{−1}$) of aromatic isomers *i* and *j* adsorbed per gram of MOF, and c_j and c_i the equilibrium concentrations (mol $L^{−1}$) of isomers *j* and *i* present in the external liquid phase. The accuracy of selectivities calculated using eq 1 decreases in cases where the relative concentration differences between solutions with and without adsorbent approach the experimental error; for instance, when uptake of one compound is very low.[38,39]

(27) Méthivier, A. In *Zeolites for Cleaner Technologies, Catalytic Science Series*; Guisnet, M., Gilson, J. P., Eds.; Imperial College Press: London, 2002; Vol. 3, pp 209−221.

(28) Kaerger, J.; Ruthven, D. *Diffusion in Zeolites*; Wiley: New York, 1992.

(29) Cottier, V.; Bellat, J.-P.; Simonot-Grange, M.-H. *J. Phys. Chem. B* **1997**, *101*, 4798–4802.

(30) Kaerger, J.; Ruthven, D. In *Handbook of Porous Solids*; Schüth, F., Sing, K., Weitkamp, J., Eds.; Wiley-VCH: Weinheim, 2002; pp 2089−2173.

(31) Kulprathipanja, S.; Johnson, J. In *Handbook of Porous Solids*; Schüth, F., Sing, K., Weitkamp, J., Eds.; Wiley-VCH: Weinheim, 2002; pp 2568−2612.

(32) Hulme, R.; Rosensweig, R.; Ruthven, D. *Ind. Eng. Chem. Res.* **1991**, *30*, 752–760.

(33) Ruthven, D.; Goddard, M. *Zeolites* **1986**, *6*, 275–282.

(34) Goddard, M.; Ruthven, S. *Zeolites* **1986**, *6*, 283–289.

(35) Ruthven, D. *Principles of Adsorption and Adsorption Processes*; Wiley: New York, 1984; p 332 and pp 401−405.

(36) Olken, M. M.; Lee, G. J.; Garces, J. M. U.S. Patent No. 4996388, 1991.

(37) Perego, C.; Ingallina, P. *Catal. Today* **2002**, *73*, 3–22.

(38) Daems, I.; Leflaive, P.; Méthivier, A.; Denayer, J.; Baron, G. *Microporous Mesoporous Mater.* **2005**, *82*, 191–199.

(39) Daems, I.; Leflaive, P.; Méthivier, A.; Denayer, J.; Baron, G. *Adsorption* **2005**, *11*, 189–194.

Pulse and breakthrough chromatographic experiments were performed at 298 K on a 5 cm stainless steel column with an internal diameter of 4 mm filled with MOF crystallites, placed in a high-performance liquid chromatography (HPLC) apparatus. For pulse experiments, 1 μL of a hexane mixture of compounds was injected into hexane flowing over the column (2 mL min^{-1} for columns filled with MIL-53*ht* and 4 mL min^{-1} for columns filled with MIL-47). A refractive index detector (RID) was connected to the column outlet. Peaks were identified by reference injections using different concentration ratios of isomers. No effect of concentration on the retention time was observed, indicating that the experiments were performed in the linear part of the isotherm. For breakthrough experiments, a binary solution of alkylaromatics in hexane was pumped over the column at 0.5 mL min^{-1}. Samples of 1 mL were taken directly at the column outlet, and concentrations were determined by GC analysis. Average selectivities were calculated from breakthrough curves using eq 1, in which the adsorbed amounts *q* were calculated using eq 2,

$$q = \int_0^t u(C_{in} - C_{out})\,dt \qquad (2)$$

with *u* the volumetric flow rate of the feed (L min^{-1}) and C_{in} and C_{out} the concentrations (mol L^{-1}) of the adsorbate in the liquid feed and eluent, respectively. After each experiment the column was regenerated using a 2 mL min^{-1} hexane flow for 2 h.

2.3. Crystal Structure Analysis. MIL-53*ht* samples used for Rietveld refinements were loaded with alkylaromatics (*o*-, *m*-, and *p*-xylene and *o*-cymene) by immersing them in pentane solutions of the specific compounds. The concentration was chosen in order to finally obtain an adsorbate loading of 35 wt %. After evaporation of pentane, the loaded MIL-53 crystallites were sealed in 0.5 mm glass capillaries (Hilgenberg). XRD experiments were performed on a Stoe Stadi P with Cu Kα_1 radiation (40 kV, 30 mA) in Debye—Scherrer geometry in a range of $0° \leq 2\theta \leq 80°$ and a step size of $0.03°$ 2θ at room temperature. The diffractometer was equipped with a curved Ge(111) monochromator and a 140°-curved image plate detector with a resolution of about 0.1° 2θ at full width at half-maximum.

Rietveld refinements were performed using the GSAS/EXPGUI software package.[40,41] The starting model was generated from the structure parameters published by Loiseau et al.[5] To account for changes of lattice parameters during adsorption, the aromatic groups in the framework were converted to rigid bodies during refinement. The guest molecules were also treated as rigid bodies. Coordinates of the rigid bodies were freely refined. Except for the sample loaded with *p*-xylene, all samples consisted of a single phase in the space group *Imma*, consistent with the MIL-53*ht* structure. The sample containing *p*-xylene consisted of two phases with symmetries corresponding to the *ht*- (*Imma*) and *as*-forms (*Pnma*), respectively. The CIF files of the refined structures are available in the Supporting Information and have also been deposited with the Cambridge Crystallographic Data Centre as CCDC-684200, CCDC-684201, and CCDC-684202 (www.ccdc.cam.ac.uk/conts/retrieving.html).

3. Results and Discussion

3.1. Adsorption of Alkylaromatics by MIL-53. Adsorption preferences of MIL-53*ht* for C$_8$ alkylaromatics were first screened with competitive batch experiments using binary solutions in hexane with a concentration of 0.014 M for each compound. The offered amount of aromatics in these experiments was theoretically able to fill the pores completely (estimated on the basis of the pore volume, as measured by N$_2$ physisorption, and the bulk density of the pure liquids). Selectivities calculated from GC data are given in Table 1. The

(40) Larson, A. C.; Von Dreele, R. B. *Los Alamos Natl. Lab. Rep.* **2004**, LA-UR-86-748.
(41) Toby, B. H. *J. Appl. Crystallogr.* **2001**, *34*, 210–213.

Table 1. Selectivities Calculated from the Uptake from 0.028 M Binary Mixtures of C$_8$ Alkylaromatic Compounds in Hexane by MIL-53[a]

	j			
i	*o*-xylene	*m*-xylene	*p*-xylene	ethylbenzene
o-xylene	−	2.7	3.5	10.9
m-xylene		−	1.2	3.8
p-xylene			−	3.1
ethylbenzene				−

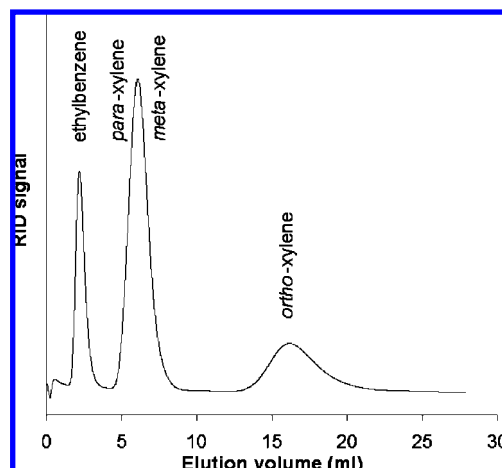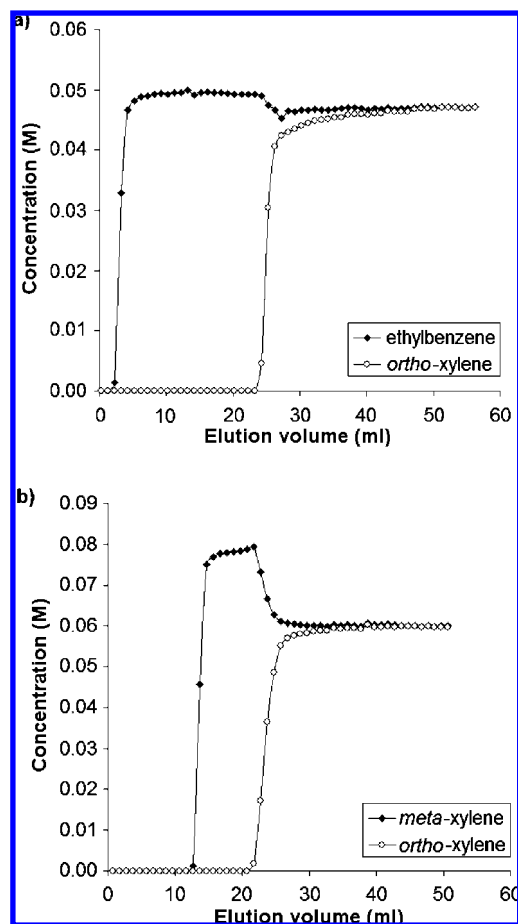[a] Batch experiments at 298 K.

Figure 1. Chromatographic separation of a mixture of C$_8$ alkylaromatics on a column packed with MIL-53*ht* crystallites and with hexane as the desorbent at 298 K. The signal intensity of the RID is shown versus the eluted volume. The curve has been corrected for dead volume.

effective uptake of aromatics varied between 1 and 9 wt %, corresponding to 0.08 and 0.7 molecules per unit cell or a relatively low degree of pore filling (<20% of the pore volume). It is clear that MIL-53*ht* has a particular preference for *o*-xylene, while ethylbenzene uptake seems to be strongly disfavored. MIL-53*ht* does not discriminate much between *m*- and *p*-xylene in these conditions. Remarkably, when unpretreated MIL-53 samples (known as MIL-53*lt*) were used in these experiments, very similar uptakes and selectivities were obtained. Hence, the interactions between the MIL-53 framework and water seem not strong enough to inhibit adsorption of aromatics. The observations in Table 1 are confirmed in a pulse chromatographic experiment (Figure 1). Ethylbenzene appears first in the eluent. Next, the joint elution of *p*- and *m*-xylene is visible as one peak, whereas *o*-xylene appears last.

The potential of MIL-53 for effective separations of C$_8$ alkylaromatics was proven by breakthrough experiments, using a 5 cm stainless steel column filled with MIL-53*ht* crystallites placed in a HPLC apparatus (see Experimental Section). A constant 0.5 mL min^{-1} flow of a 0.047 M solution of aromatics was pumped over the column. This concentration was chosen to obtain a relatively high degree of pore filling with the aromatics. Thus, the conditions are different from those of the pulse chromatographic experiments, which were performed in the linear, low-concentration part of the isotherm. The column outlet was manually sampled and afterward analyzed by GC. In this way, breakthrough profiles are obtained, as shown in Figure 2a for *o*-xylene and ethylbenzene. Ethylbenzene appears in the column outlet after a very short time. During a long time interval, only ethylbenzene elutes from the column, at a slightly higher concentration than its inlet concentration. Next, the breakthrough of *o*-xylene is observed after elution of 24 mL of

Figure 2. Breakthrough experiments with binary solutions of C$_8$ alkylaromatic compounds in hexane on a column filled with MIL-53*ht* crystallites at 298 K: effluent concentrations of (a) *o*-xylene and ethylbenzene (inlet concentrations, 0.047 M) and (b) *o*- and *m*-xylene (inlet concentrations, 0.060 M) as a function of the eluted volume. The experiments were performed on different columns. The curves have been corrected for dead volume.

Figure 3. Competitive batch adsorption experiments on MIL-53: uptake (MPUC = number of molecules per unit cell; Q = weight percentage) from (a) a mixture of *o*- and *p*-xylene and (b) a mixture of *o*-xylene and ethylbenzene in hexane as a function of the total equilibrium bulk phase concentration of both compounds. Selectivities α calculated from the data points are given on the right axis.

solvent. At this point, the ethylbenzene concentration decreases to its inlet value, and after a while the two curves coincide. From integration of the complete breakthrough profiles, an average apparent selectivity of $\alpha_{oX,EB} = 11.0$ was calculated. A similar breakthrough curve is obtained with a mixture of *o*- and *m*-xylene (Figure 2b). The higher affinity of MIL-53 for *o*- and *m*-xylene compared to ethylbenzene is clear from the much longer time interval during which both compounds are fully adsorbed by MIL-53. The roll-up of *m*-xylene in Figure 2b is much more pronounced than that of ethylbenzene in Figure 2a. The higher intraporous concentration of *m*-xylene compared to that of ethylbenzene results in a larger increase in effluent concentration as soon as *o*-xylene starts to displace the more weakly adsorbed *m*-xylene from the column. The average apparent selectivity calculated from the curves shown in Figure 2b is $\alpha_{oX,mX} = 2.2$. It can be expected that the separation performance and the shape of the breakthrough curves are affected by the concentration of the aromatics in the hexane feed. A pronounced effect of the degree of pore filling on the dynamic separation of C$_8$ alkylaromatics was recently found for MIL-47.[42] Such a detailed study is outside the scope of the present work; instead, the effect of pore filling on selectivity was further studied in batch mode.

In Figure 3, competitive adsorption is shown as a function of the equilibrium external bulk phase concentration. When *o*-
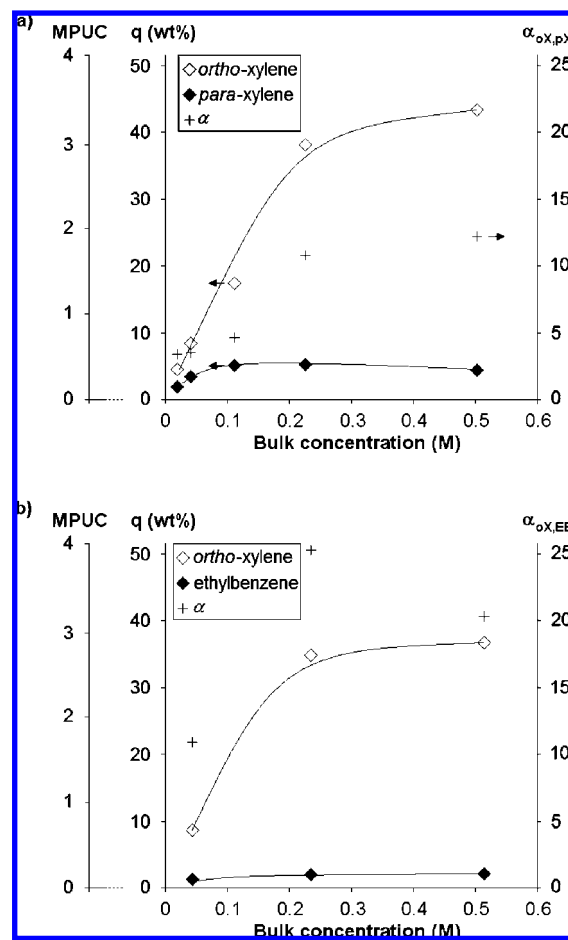
and *p*-xylene are co-adsorbed, uptake of *p*-xylene is never higher than 5 wt % (0.4 molecule per unit cell), while *o*-xylene adsorption increases up to a plateau of 45 wt % (3.5 molecules per unit cell) (Figure 3a). These trends are reflected in an increasing selectivity α between the two isomers. Additionally, similar developments are observed in the co-adsorption of *o*-xylene and ethylbenzene (Figure 3b). The very low affinity of MIL-53 for ethylbenzene is clear from the uptakes, which are never higher than 2 wt %. In both figures, the strongly increasing adsorption preference for *o*-xylene at increasing external bulk phase concentration indicates that this isomer is packed more easily inside the pores. This was confirmed by room-temperature isotherms for the adsorption of the individual C$_8$ alkylaromatic compounds from a hexane solution (Figure 4). The adsorption isotherm of *o*-xylene rises steeply and quickly reaches a plateau at 46 wt %, while the rise of the other isotherms is more gradual. The isotherms of *m*-xylene and ethylbenzene do not reach a plateau in the tested concentration range. At concentrations below 0.12 M, the relative positions of the adsorption isotherms are in accordance with the order of preference found in the competitive batch experiments, carried out in this same concentration range (see Table 1), and with

(42) Finsy, V.; Verelst, H.; Alaerts, L.; De Vos, D.; Jacobs, P.; Baron, G.; Denayer, J. *J. Am. Chem. Soc.* **2008**, *130*, 7110–7118.
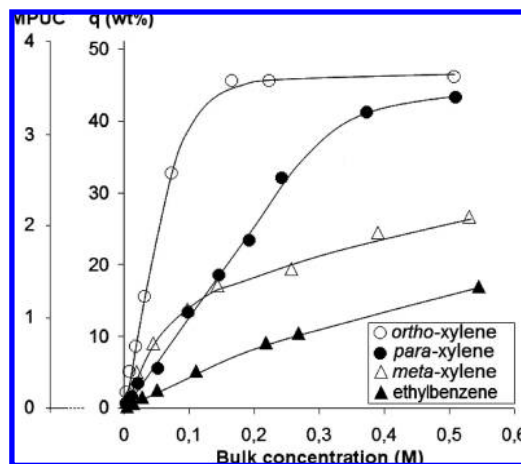
Figure 4. Single-compound adsorption isotherms on MIL-53 measured in batch mode at 298 K: uptake (MPUC = number of molecules per unit cell; Q = weight percentage) of C_8 alkylaromatic compounds from hexane as a function of the equilibrium bulk phase concentration.

Table 2. Selectivities Calculated from the Uptake from 0.028 M Binary Mixtures of Ethyltoluene Isomers in Hexane by MIL-53[a]

	j		
i	*o*-ethyltoluene	*m*-ethyltoluene	*p*-ethyltoluene
o-ethyltoluene	−	4.7	5.5
m-ethyltoluene		−	1.0
p-ethyltoluene			−

[a] Batch experiments at 298 K.

Table 3. Selectivities Calculated for the Uptake from 0.028 M Binary Mixtures of Cymene Isomers in Hexane by MIL-53[a]

	j		
i	*o*-cymene	*m*-cymene	*p*-cymene
o-cymene	−	4.6	7.1
m-cymene		−	2.4
p-cymene			−

[a] Batch experiments at 298 K.

the pulse chromatographic experiments (Figure 1). The curve for *p*-xylene is remarkable. It gradually approaches the curve for *m*-xylene, crosses it at external concentrations between 0.10 and 0.15 M, and keeps rising up to a plateau at the highest measured concentrations, not far below the plateau of *o*-xylene. Thus, the adsorption preference between *p*- and *m*-xylene changes with concentration; *m*-xylene is preferred at low concentration and *p*-xylene at high concentration. Such an effect could be due to a change in the lattice parameters of MIL-53 upon adsorption of *p*-xylene,[5] but also to a more efficient stacking of *p*-xylene at higher intraporous concentrations (vide supra).

The same experimental approach was used to investigate the adsorption of the larger ethyltoluene and cymene isomers. Selectivities calculated from competitive batch adsorption experiments are shown in Tables 2 and 3. The order of preference of the three isomers is similar to the order observed for the C_8 alkylaromatics, with again a very striking preference for the *ortho*-isomer. For the ethyltoluene isomers, the effective uptake varied between 1 and 5 wt % (0.07 and 0.35 molecule per unit cell), while uptake of cymene isomers was never higher than 2.5 wt % (0.16 molecule per unit cell) at the low concentrations offered. Hence, keeping the external concentration constant, the intraporous concentration of aromatics pro-
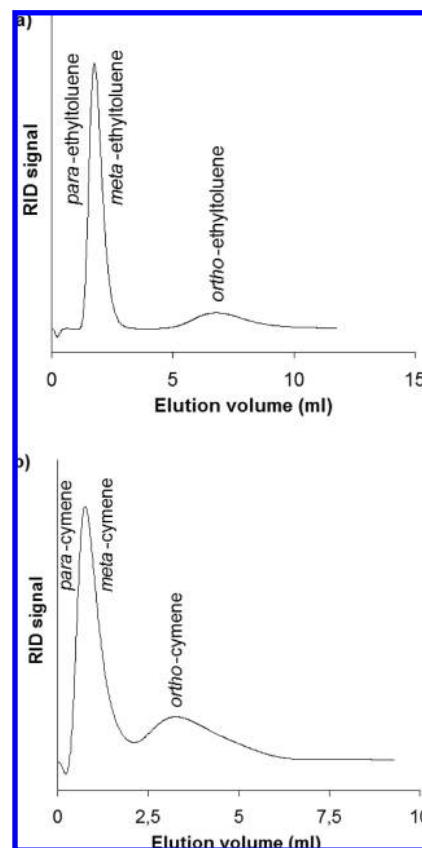

Figure 5. Chromatographic separation of a mixture of (a) ethyltoluene isomers and (b) cymene isomers on a column packed with MIL-53*ht* crystallites and with hexane as the desorbent at 298 K. The signal intensity of the RID is shown versus the eluted volume. The curves have been corrected for dead volume of the column.

gressively decreases as a function of the number of carbon atoms of the adsorbates (see also xylene uptake). This illustrates the increasing difficulty of positioning larger aromatics inside a sterically confining space. However, the *ortho*-compounds, which are most preferred, do not have the smallest dimensions in comparison with their respective *meta*- and *para*-isomers, showing that their selective uptake is certainly not caused by a shape-selective molecular sieving effect. The adsorption preferences found in pulse chromatographic experiments (Figure 5) using a column filled with MIL-53*ht* crystallites are in accordance with the data listed in Tables 2 and 3. The *ortho*-isomer elutes each time significantly later than the other isomers, the peaks of which are not separated from each other. The very fast elution of *p*- and *m*-cymene indicates low affinity of MIL-53 for these compounds.

The potential of MIL-53 to separate these isomers was tested with breakthrough experiments (Figure 6). The lower affinity for ethyltoluene and cymene isomers can be seen in the faster breakthroughs of these compounds in comparison with the profiles of the xylenes studied in Figure 2. A roll-up is still clearly observed for the cymene isomers, but it is less pronounced than for the ethyltoluenes. This agrees with the low affinity of MIL-53 for *p*- and *m*-cymene. The elution of *p*-cymene in Figure 6 takes place very shortly after the elution of the dead volume. By integration of the curves in Figure 6, average apparent selectivities were calculated, with values of $\alpha_{o,m} = 5.0$ for the ethyltoluene isomers and $\alpha_{o,p} = 6.8$ for the cymene isomers.
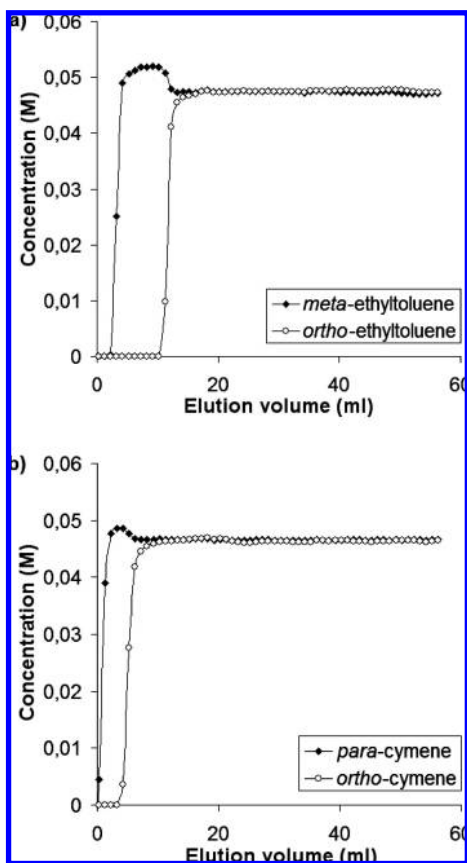
Figure 6. Breakthrough experiments with binary 0.047 M solutions of (a) *o*- and *m*-ethyltoluene and (b) *o*- and *m*-cymene in hexane on a 5 cm column filled with MIL-53*ht* at 298 K: effluent concentrations as a function of the eluted volume. The curves have been corrected for the dead volume of the column.

Figure 7. Competitive batch adsorption experiments on MIL-53: uptake (MPUC = number of molecules per unit cell; *Q* = weight percentage) from (a) a mixture of *o*- and *m*-ethyltoluene and (b) a mixture of *o*- and *p*-cymene in hexane as a function of the total equilibrium bulk phase concentration of both compounds. Selectivities α were calculated only for the ethyltoluene isomers and are given on the right axis.

The concentration dependence of the observed selectivities was also investigated with competitive batch experiments at increasing external bulk phase concentrations, as shown in Figure 7. In the case of competitive *o*- and *m*-ethyltoluene adsorption (Figure 7a), the uptake of both compounds increases steadily up to 35 wt % at the highest loadings, corresponding to 2.4 molecules per unit cell. No plateaus are reached in the tested concentration range. The selectivity varies between 3.7 and 4.7, without a clear decrease or increase over the measured concentration range. In the case of the cymene isomers (Figure 7b), uptake of *p*-cymene is no longer detected beyond an external concentration of 0.14 M, and hence selectivities were not calculated. Uptake of *o*-cymene increases and the curve moves toward a plateau at ca. 10 wt % (0.6 molecule per unit cell), which is a much lower value in comparison with *o*-xylene or *o*-ethyltoluene uptake at high external concentration.

3.2. Rietveld Refinements. Samples of MIL-53*ht* were loaded with xylene isomers (see Experimental Section). Changes in the MIL-53 structure during adsorption were analyzed by Rietveld refinements of XRD data sets (see Supporting Information). Besides the position of the adsorbates in the pores of MIL-53 (Figure 8), structure analysis also revealed that the lattice parameters vary significantly after adsorption of alkylaromatics (Table 4). Upon adsorption of *o*-xylene, the obtuse angle between opposing terephthalate ligands is reduced from 104.9° for an empty MIL-53*ht* structure to 97.8°, which is a stronger deformation of the channels compared to the effects of adsorption of the *meta*- or *para*-isomer (see Table 4). The *para*-isomer
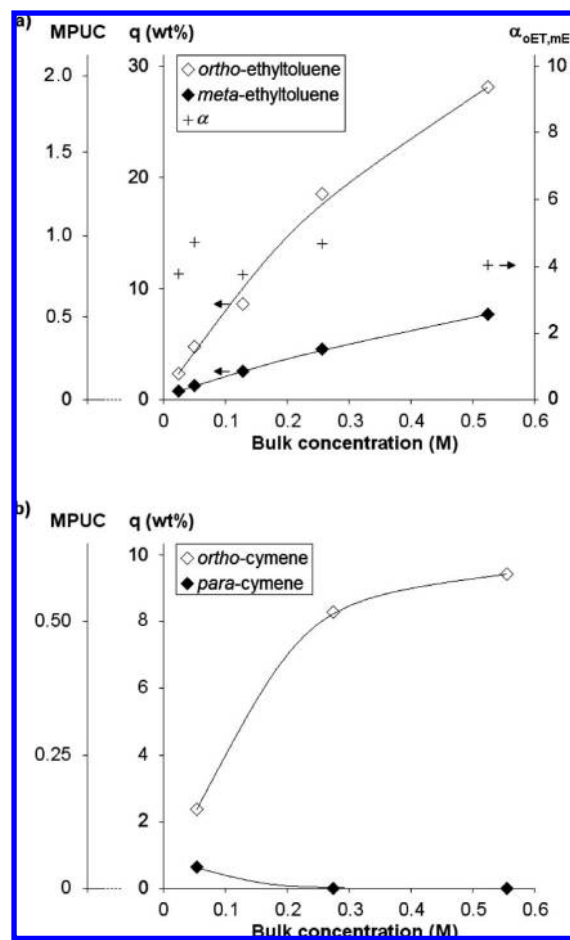
distorts the framework in *Imma* symmetry to a lesser extent than the other xylene isomers, indicating that the interaction between the lattice and this molecule is the weakest. These observations closely mirror the observed selectivities, at least at low concentrations (Table 1). All positions of the investigated guest molecules in the MIL-53*ht* structure have in common that at least one methyl group is found in the vicinity of the carboxylate groups of two opposing terephthalate framework ligands (Figure 8). The molecular geometry of *o*-xylene allows the interaction of both methyl groups with the carboxylate groups of the framework. *m*- and *p*-xylene molecules can only interact with the carboxylate groups via one methyl group simultaneously. However, the methyl group in the *meta*-position and the C2 carbon atom of the aromatic ring of *m*-xylene are found within interaction distance of an aromatic ring of the host. The geometry of *p*-xylene prevents interaction of both methyl groups with the framework.

For both *o*- and *m*-xylene, the refined molecule positions have four symmetry-equivalent sites in the obtuse pore corner formed by two opposing terephthalate carboxylate groups, the simultaneous occupation of which is prevented by steric constraints (see Supporting Information). If each of the obtuse corners is occupied by one molecule, maximally one molecule per Al-atom can be adsorbed in the *ht*-form, or four molecules per unit cell. This corresponds to a theoretical value of 55 wt %, which
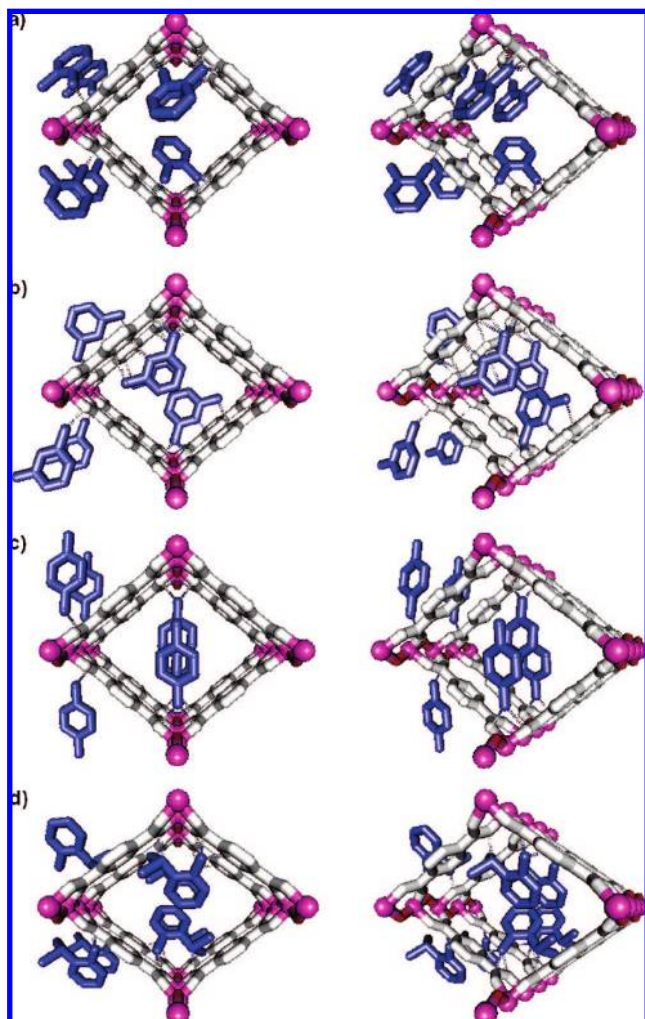
Figure 8. Structure refinements of MIL-53*ht* crystals loaded with alkylaromatic isomers: packing in the pores of (a) *o*-xylene, (b) *m*-xylene, (c) *p*-xylene, and (d) *o*-cymene.

Table 4. Lattice Constants and Rhombic Channel Angles of the Unloaded *ht* and *as* Structures from the Literature and of the Alkylaromatic-Loaded MIL-53 Structures Determined from X-ray Powder Diffraction Data via Rietveld Refinement[a]

MIL-53	space group	a/Å	b/Å	c/Å	rhombic channel angle/°
ht structure[b]	*Imma*	6.6085(9)	16.675(3)	12.813(2)	104.92
o-xylene	*Imma*	6.63098(22)	15.9473(7)	13.9205(6)	97.76
m-xylene	*Imma*	6.63456(28)	16.0005(8)	13.8726(7)	98.15
p-xylene[c]	*Imma*	6.622(2)	16.215(2)	13.588(2)	100.79
o-cymene	*Imma*	6.63378(22)	16.2884(6)	13.4909(5)	100.73
as structure[b]	*Pnma*	17.129(2)	6.6284(6)	12.1816(8)	
p-xylene[c]	*Pnma*	16.241(5)	6.635(1)	13.495(3)	

[a] The numbers in parentheses are the estimated standard deviations of the lattice constants, based on the goodness of fit and statistics of the Rietveld refinement. [b] Values from ref 5. [c] Two phases were found for the *p*-xylene loaded samples.

comes reasonably close to the plateau in the *o*-xylene adsorption isotherm (Figure 4). As the overall symmetry of the framework still is well described by the *Imma* space group, either static or dynamic disorder of molecules over these four sites has to be assumed. Most probably the availability of four equivalent adsorption sites has a favorable effect on the guest−host system in terms of entropy.

For samples loaded with *p*-xylene, two phases were found. In addition to the phase with space group *Imma*, also a MIL-53 phase with *Pnma* symmetry was present, which is the same space group as MIL-53*as*. Despite the considerable overlap of reflections of the two phases, the localization of the guest molecules in the *Imma* phase readily converged on one site, leading also to reasonable temperature factors. Even with a conservative treatment of the data due to the presence of two phases, the occupation factors for *p*-xylene in the MIL-53*ht* phase turned out to be high: the loading approaches four molecules per unit cell, which is again expected on the basis of the plateau in the sorption isotherm for *p*-xylene-loaded MIL-53*ht* (Figure 4). The positioning of the *p*-xylene molecules allows lateral interactions between the methyl group of one *p*-xylene molecule and the π-system of an adjacent *p*-xylene molecule. Similar arrangements of the π-system and a methyl group are, for instance, also found in the crystal structure of *p*-xylene itself[43] and in *p*-xylene-loaded silicalite.[44] The increasing affinity of MIL-53 for *p*-xylene at higher intraporous concentrations (Figure 4) may then be explained by favorable adsorbate−adsorbate interactions which become possible only when adsorbed *p*-xylene molecules are close to each other. Note that similar interactions do not occur for the *ortho*- and *meta*-isomers since both of their methyl groups already interact with the MIL-53 framework at high degrees of pore filling, as can be perceived from Figure 8. Regarding the second MIL-53 phase with the *Pnma* space group, we failed to precisely localize *p*-xylene in this phase. Molecule positions did not converge onto a specific site. From inspection of difference electron Fourier charts, no considerable electron density due to guest molecules anywhere close to the framework was found. This suggests that this phase contains only a low concentration of *p*-xylene, and that it is formed when MIL-53*ht* is exposed to a small dose of *p*-xylene. Only when the *p*-xylene concentration is increased is the *Imma* MIL-53 phase with interacting *p*-xylene molecules formed.

Next, *o*-cymene was localized in the host to see whether the strong adsorption of the C_9 and C_{10} *ortho*-isomers can be ascribed to their ability to interact via two side chains simultaneously. Here also, the refined molecule positions have four symmetry-equivalent sites that cannot be simultaneously occupied for steric reasons. Surprisingly, the bulky isopropyl group does not prevent the interaction between the carboxylate groups of the host and the two C−H groups in the α-position of the aromatic ring. The smaller distortion of the MIL-53 lattice confirms that the interactions with this compound are weaker than the interactions with the less bulky xylenes. For the other cymene isomers, and also for the ethyltoluene isomers, interactions similar to those found for xylene adsorption are likely operative. Thus, the *para*-isomers can interact at only one site in the pore corner, while the *meta*-isomers might establish additional interactions with the aromatic rings of the framework.

3.3. Adsorption of Alkylaromatics by MIL-47. An interesting comparison can be made between the alkylaromatics adsorption on MIL-53 and on the isotypical metal−organic framework MIL-47. The pore architectures of these materials are similar. An in-depth study covering the adsorption of C_8 alkylaromatics

(43) Van Koningsveld, H.; Van Den Berg, A. J.; Jansen, J. C.; De Goede, R. *Acta Crystallogr.* **1986**, *B42*, 491–497.
(44) Van Koningsveld, H.; Tuinstra, F.; Van Bekkum, H.; Janssen, J. *Acta Crystallogr.* **1989**, *B45*, 423–431.

on MIL-47 has been presented in earlier work.[42,45] In that study, the affinity of MIL-47 for xylene isomers was shown to be largely determined by the packing efficiency. In the vapor phase, at a low degree of pore filling, all C_8 alkylaromatics have the same adsorption strength and adsorb unselectively on MIL-47. With increasing degree of pore filling, selectivity develops because the ease with which the molecules can be densely packed in the MIL-47 pores differs among the isomers. The possibility to establish $\pi-\pi$ interactions between the aromatic rings of two adsorbate molecules and steric constraints imposed by the framework both play important roles in the packing mechanism. On MIL-47, o- and p-xylene were preferred much more than m-xylene or ethylbenzene, and efficient separations of p- and m-xylene as well as of p-xylene and ethylbenzene could be achieved, with selectivities of 2.9 and 9.7, respectively, under the same conditions as those given in Table 1. These separation factors become even larger at higher alkylaromatics concentrations. Also in the present study of MIL-53(Al), the selectivity between the isomers increases with alkylaromatics concentration and thus degree of pore filling with aromatics (see Figure 3), but different selectivity patterns are obtained. The selectivity at low C_8 alkylaromatics concentration decreases in the order o-xylene > m-xylene > p-xylene. This order of selectivity is governed by the strength of interaction: o-xylene is capable of interacting via both of its methyl groups with carboxylate groups of the framework; m-xylene interacts via one methyl group with one carboxylate group, but also via the second methyl group and the C2 carbon atom of the aromatic ring with an aromatic ring of the host. p-Xylene finally has only a specific interaction between one of its methyl groups and a framework carboxylate group. These specific interactions between methyl groups of the adsorbates and carboxylate groups of the MIL-53 adsorbent are not present in MIL-47.

The observed increase in selectivity with bulk concentration or degree of pore filling typically points at a separation mechanism in which molecular packing plays an important role.[46-49] For separations that are purely based on differences in interaction strength, the selectivity typically decreases with pore filling since, in the first instance, the most selective sites are occupied and the less selective sites are only occupied at higher degrees of pore filling. In order to increase the amount of C_8 alkylaromatic compounds in the MIL-53 pores and thus replace the hexane solvent molecules, obviously an increase in bulk phase concentration is required. The larger the energetic interaction of the molecules with the framework at a high degree of pore filling, the more easily the molecules can be packed. Interestingly, p-xylene reaches a dense packing state at much lower concentrations than m-xylene, in spite of a lower uptake at low concentration (see Figure 3). This effect is explained by the occurrence of lateral interactions between the methyl group of one p-xylene molecule and the π-system of an adjacent p-xylene molecule at high degrees of pore filling, which lowers the energy cost to fill the pores.

MIL-53 and MIL-47 were further compared for adsorption of ethyltoluene isomers. Selectivities calculated from competitive

(45) Alaerts, L.; Kirschhock, C.; Maes, M.; van der Veen, M.; Finsy, V.; Depla, A.; Martens, J.; Baron, G.; Jacobs, P.; Denayer, J.; De Vos, D. *Angew. Chem., Int. Ed.* **2007**, *46*, 4293–4297.
(46) Krishna, R.; van Baten, J. *Sep. Purif. Technol.* **2008**, *60*, 315–320.
(47) Dubbeldam, D.; Calero, S.; Maesen, L. M.; Smit, B. *Angew. Chem.* **2003**, *115*, 3752–3754; *Angew. Chem., Int. Ed.* **2003**, *42*, 3624–3626.
(48) Talbot, J. *AIChE. J.* **1997**, *43*, 2471–2478.
(49) Ruthven, D.; Loughlin, K.; Holborow, K. *Chem. Eng. Sci.* **1973**, *28*, 701–709.

Table 5. Selectivities Calculated for the Uptake from 0.028 M Binary Mixtures of Ethyltoluene Isomers in Hexane by MIL-47[a]

i	j		
	o-ethyltoluene	m-ethyltoluene	p-ethyltoluene
o-ethyltoluene	−	1.8	1.1
m-ethyltoluene		−	0.5
p-ethyltoluene			−

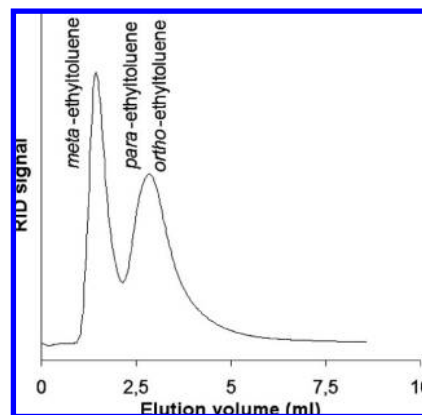[a] Batch experiments at 298 K.

Figure 9. Chromatographic separation of a mixture of ethyltoluene isomers on a column packed with MIL-47 and with hexane as the desorbent at 298 K. The signal intensity of the RID is shown versus the eluted volume. The curve has been corrected for the dead volume of the column.
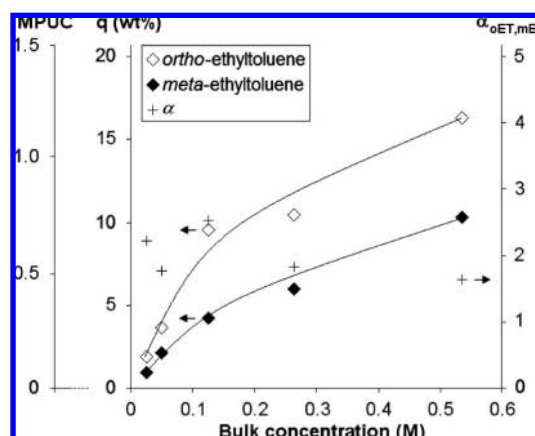

Figure 10. Competitive batch adsorption experiments on MIL-47: uptake (MPUC = number of molecules per unit cell; Q = weight percentage) from a mixture of o- and m-ethyltoluene in hexane as a function of the total equilibrium bulk phase concentration of both compounds. Selectivities α calculated from the data points are given on the right axis.

batch experiments on MIL-47 are shown in Table 5. The experimental conditions were identical to those used for the experiments listed in Table 2. The effective uptake of aromatics varied between 2 and 4 wt %. o- and p-ethyltoluene are almost equally preferred by MIL-47 and are more strongly retained than m-ethyltoluene. These selectivities are confirmed in a pulse chromatographic experiment using a column filled with MIL-47 crystallites (Figure 9). In comparison with MIL-53, uptakes and selectivities are lower and the preference orders differ. Adsorption of ethyltoluene isomers on MIL-47 was further studied with competitive batch experiments at increasing external bulk phase concentrations of o- and m-ethyltoluene (Figure 10). Uptake of both compounds steadily increases, but no increase in selectivity is observed upon increasing the concentration. When solutions of cymene isomers were con-

tacted with MIL-47, uptakes were never higher than 1 wt % in batch experiments similar to those used to obtain the results listed in Table 3. In a pulse chromatographic experiment with all three cymene isomers, a chromatogram with a single peak eluting very shortly after the dead volume is obtained, pointing to poor interaction of the cymene isomers with MIL-47.

Thus, despite having almost identical pore topography, MIL-53 and MIL-47 display very different selectivities and interaction mechanisms. It could be expected that the presence of different metals in the two materials might lead to a different polarization of the carboxylate groups, which in turn affects the strength of interaction with the adsorbates, enabling interactions between the carboxylate groups of the MIL-53 lattice and the adsorbates. These specific interactions lead to a different orientation of the molecules compared to MIL-47 and, as a result, different packing modes. Variation in polarity in porous systems has previously been observed to have a strong effect on selectivity. A similar case is encountered in the family of Faujasite zeolites, where materials with the same pore topography but different types and numbers of cations show an astonishing variety of selectivity between C_8 alkylaromatics.[27] In the systems studied here, the pores vary not only in polarity but also in their flexibility, which results in a remarkable diversity of guest−host interactions.

Conclusion

In this work, adsorption of C_8, C_9, and C_{10} alkylaromatics on MIL-53(Al) has been investigated with an experimental approach consisting of a combination of batch and column experiments. In all experiments, MIL-53 has a pronounced preference for the *ortho*-isomers. In the case of the xylenes, molecular packing clearly plays an important role; the preferences found among the isomers are determined by interactions of the methyl groups with the pore walls. Comparing molecule localizations from Rietveld refinements with adsorption prefer-

ences, the strongest interactions are found between methyl groups of the adsorbates and carboxylate moieties in the obtuse pore corners. Other but weaker interactions may be established with the aromatic rings of the lattice, depending on the relative position of the second substituent. This explanation seems valid also for adsorption of ethyltoluene and cymene isomers. Steric factors become increasingly important for these adsorbates. Their larger size most probably decreases the number of possible and preferred coordination sites, resulting in weaker interactions and lower uptakes under the same experimental conditions. Notably, when the same adsorption experiments as for the MIL-53 samples are carried out with MIL-47 as adsorbent, completely different adsorption preferences are obtained. The results presented in this work should encourage further efforts to investigate the use of MOFs as adsorbents for larger molecules. Considering the current flood of new MOF structures with often intriguing pore topologies, there is no doubt that MOFs will eventually find real applications in industrial separation processes or environmental technologies. For instance, it is demonstrated in this work that MIL-53 could be readily used to selectively retain the *ortho*-compounds from a feed of alkylaromatic isomers.

Supporting Information Available: Refined X-ray powder diffraction patterns, CIF files, and 3D animations (as VRML files) of the MIL-53 structures loaded with xylene isomers and *o*-cymene; animated GIF files showing the symmetry equivalent sites of the xylenes in MIL-53. This material is available free of charge via the Internet at http://pubs.acs.org.

JA802761Z